Original Research Article: full paper

(2023), «EUREKA: Physics and Engineering»
Number 1

COMBINED ANALYSIS OF ACOUSTIC EMISSION AND VIBRATION SIGNALS IN MONITORING TOOL WEAR, SURFACE QUALITY AND CHIP FORMATION WHEN TURNING SCM440 STEEL USING MQL

Dung Hoang Tien✉
Faculty of Mechanical Engineering[1]
tiendung@haui.edu.vn

Nguyen Van Thien
Department of General Administration[1]

Thoa Thi Thieu Pham
Faculty of Mechanical Engineering[1]

Trinh Duy Nguyen
Faculty of Mechanical Engineering[1]

[1]*Hanoi University of Industry*
298 Cau Dien str., Bac Tu Liem District, Hanoi, Vietnam, 100000

✉**Corresponding author**

Abstract

With modern production, Minimum Quantity Lubricant (MQL) technology has emerged as an alternative to conventional liquid cooling. The MQLs is an environmentally friendly lubricant method with low cost while meeting the requirements of machining conditions. In this study, the experimental and analytical results show that the obtained acoustic emission (AE) and vibration signal components can effectively monitor various circumstances in the SCM440 steel turning process with MQL, such as surface quality and chip formation as cutting tool conditions. The AE signals showed a significant response to the tool wear processes. In contrast, the vibration signal showed an excellent ability to reflect the surface roughness during turning with MQL. The chip formation process through the cutting mode parameters (cutting speed, feed and depth of cut) was detected through analysis amplitude of the vibration components *Ax*, *Ay* and *Az* and the AE signal. Finally, Gaussian process regression and adaptive neuro-fuzzy inference systems (GPR-ANFIS) algorithms were combined to predict the surface quality and tool wear parameters of the MQL turning process. Tool condition monitoring devices assist the operator in monitoring tool wear and surface quality limits, stopping the machine in case of imminent tool breakage or lower surface quality. With the unique combination of AE and vibration analysis model and the training and testing samples established by the experimental data, the corresponding average prediction accuracy is 97.57 %. The highest prediction error is not more than 3.8 %, with a confidence percentage of 98 %. The proposed model can be used in industry to predict surface roughness and wear of the tools directly during turning.

Keywords: acoustic emission, vibration signal, tool wear, surface quality, chip formation.

DOI: 10.21303/2461-4262.2023.002509

1. Introduction

SCM440 steel has been widely used in manufacturing parts with variable loads such as motor drives, gears, plastic injection moulds, rolling shafts and other fields due to its excellent mechanical properties and ability to resist corrosion [1, 2]. However, SCM440 steel is classified as difficult-to-machine steel, causing vibrations and rapid tool wear in the machining process [3, 4]. SCM440 steel processing shows the effects of different technological parameters on surface quality and vibration [5, 6]. Many studies on milling SCM440 steel aimed to investigate the technological parameters affecting the surface quality as well as the tool life [7, 8]. Studies on machining SCM440 steel are mainly applied to cool studies with conventional cooling solutions, showing that cutting fluid benefits temperature reduction and productivity improvement [9, 10]. However, using a large amount of cutting fluid will adversely affect the environment and the operator's health.

Along with that, the solution treatment after machining also incurs high costs. Therefore, now some researchers have tried to replace cutting fluids with new cooling methods that are safer, more effective, cost-saving, and more environmentally friendly. Among them, minimum quantity lubrication (MQL) machining is considered the most efficient alternative, with a small amount of lubricant spraying to reduce friction between the workpiece and the tool. According to previous studies' results, MQL can create thin films that enhance lubricity and improve surface quality [11, 12]. Studies by [13] show that machining under MQL conditions reduces tool wear and vibration amplitudes by 23 % and 45 %, respectively, compared with dry machining. Most previous studies focused on surface roughness and tool wear by the MQL machining process. However, the systematic experimental approaches and correlations of acoustic emission signal, vibration amplitude and surface quality, and chip formation according to the MQL turning process have not been fully reported.

Smart production in industry 4.0 is an inevitable trend of production processes, with the help of smart production processes that reduce costs, reduce obliteration and further improve production efficiency through optimization and automation processes [14, 15]. A key component of smart manufacturing success is an effective process monitoring mechanism that identifies defects and suboptimal operating conditions in manufacturing and processing environments due to unforeseeable unexpected events. When changing cutting conditions and different phenomena appear to complicate the machining process in machining processes. Therefore, monitoring the cutting tool condition and surface quality without the support of sensor monitoring devices will be very difficult. Surface quality expressed through surface roughness is a significant factor in machining. Speaking product quality through surface quality also indirectly indicates the condition of the cutting tool [8, 16, 17]. In which the cutting mode parameters have a significant influence on the surface quality and tool wear. Besides that, these factors affected the plastic deformation, stability workpiece, and the cracks formed inside the workpiece. Tool wear is an ineviTable phenomenon in any metal cutting process. When the cutting edge is worn, it will increase the friction between the tool and the workpiece, resulting in increased cutting heat, cutting force, and power consumption. When the cutting tool wears out beyond the allowable range or is damaged, it will create low-quality machined surfaces and cause vibrations for technology systems. Changing cutting conditions and other machining problems also generate different vibration signals in the technology system. Analyzing the vibration signal makes it possible to identify abnormalities in the machining process and detect errors caused by the machine tool itself. Problems during machining generate vibrations that will result in increased tool wear and surface roughness. Effectively determining the condition of the cutting tool will be determined through the progress of tool wear and surface roughness during machining. The investigation of surface quality is affected by vibration and chip formation. Undesirable factors during machining become functional process parameters by monitoring tool wear and machined surface quality. In machining processes, mechanical materials are changed due to the workpiece and cutting tool interaction. This process will generate acoustic emission waves and propagate through the contact object. As a result, acoustic emission measurement enhances tool wear monitoring and surface quality, thereby further enhancing monitoring when combined with vibration and chip formation measurement.

The process combines analysis of AE and vibration signals with chip formation investigation, providing the ability to reliably determine the cutting tool conditions without interrupting the machining process. The frequency analysis components of the AE signal characterized by high frequencies represent the internal changes of the material, while the obtained vibration amplitudes characterized by low frequencies show the external changes of the material machining process, thereby showing that the combination of these two sensors creates a more comprehensive tool condition monitoring process.

Based on the above analyses, this study develops a system to monitor the tool condition and evaluate the surface quality through vibration signal, chip formation and acoustic emission experiments with an acoustic emission sensor. A three-component accelerometer captured the acoustic emission signal and vibration amplitude generated during the MQL turning SCM440 steel. The signals obtained from the AE sensor and the three-component vibration signal are time-domain signals, transforming to the frequency domain through FFT analysis. Different signals received through frequency analysis correlated with the varying tool and surface quality conditions.

2. Materials and methods

With the rapid development of sensors, real-time information on the machining process and cutting tool conditions are collected, thereby quickly detecting and avoiding serious tool failures during machining. Selecting the available and suiTable sensor types is important with cutting tool condition monitoring. Among the various types of cutting tool monitoring types, acoustic emission (AE) sensors can accurately detect cutting tools. Anomalies because these sensors receive high frequencies and are not subject to interference by ambient noise. Acoustic emission signals are instantaneous signals produced by the rapid release of energy from a local source or a source within the material. AE signal sources generating from stress caused by material deformation during metal cutting, such as Plastic deformation of the workpiece during cutting. Friction between the workpiece and the tool flank leads to flank wear. Chip forming process and chip removal; Frictional contact between the front face of the tool and the chip leads to wear of the front face. The impact between chip and tools, chip breakage, and the means is chipped or broken. The AE signals obtained from the metal cutting process are composed of continuous and instantaneous signals, which have distinct and different characteristics. Continuous AE signals are associated with plastic deformation and tool wear during metal cutting, while transient signals observing during internal crack development. In addition, chip breaking, tool breakage or breakage, chip impact or chip entanglement produce transients type AE signals. Several researchers have shown that AE has been successfully used in experimental tests to detect instrument conditions such as breakage and tool wear.

On the other hand, with the ability to quickly collect and interpret data, vibration signals have been of interest and widely used in cutting tool condition monitoring. The vibrations in metal cutting are generated by cyclic variations in the dynamic components of the cutting force. Usually, vibrations will produce tiny squeaks that cause undulations in the machined surface and irregularities in chip formation, which in turn affect the stability of the machining process. The vibration signal generated during metalworking is due to a combination of free faces, cutting forces, and periodic and random oscillations. The mechanical vibrations result from cutting conditions and tool wear during machining. Chipping and breaking of the cutting tool, interruption of machining, and other conditions related to the machining process are also causes of random vibration during machining. A minimal vibration from the machine tool, the machine next to it, and the workshop platform also incorporate vibration detection. Studies by [18] show that the tendency of these vibration components is little changed and is considered unchanged under different cutting conditions. The main conclusions of the study [18] show that the minimum vibration amplitude can be used as an indicator of tool wear and can be used in online monitoring of tool conditions. The use of vibration sensors in cutting tool condition monitoring offers several advantages over other sensors, such as ease of implementation and no need to modify jigs, workpieces and machine tools. The vibrator sensors can work well in the presence of coolant, chip, and heat and can be easily replaced, thereby saving costs.

The CMS440 steel workpieces have a diameter of 80 mm and a length of 200 mm with the chemical composition as shown in **Table 1**. The turning experiment was performed on a DMG Mori CLX350 lathe with a maximum power and spindle speed of 16.5 kW and 5000 rpm, respectively. The description in **Fig. 1** shows an image of the experimental equipment with MQL set up on a CNC lathe with an eco-friendly vegeTable oil lubricant. The vibration device by a Brüel & Kjær three-component accelerometer. Vibration data is recorded during the entire machining process. The time-domain signal data is processed as root-mean-squared (RMS) values to determine vibration intensity. Surface quality and tool wear by the roughness measuring (Mitutoyo SJ-200) and Keyence VHX device as depicted in **Fig. 2**. The average Ra value measured at three other locations on the workpiece is used as surface roughness data to ensure measurement accuracy. Experiments were conducted through experimentation on factors including cutting speed (V), feed rate (f), injection pressure and depth of cut (t) is set up on three levels. The experimental process's initial parameters are shown in **Table 2**. In order to verify the ability to predict surface quality and tool wear through the combined use of AE and vibration sensors, the experimental parameters are listed in **Table 3** with measured values through surface roughness and AE frequency and

amplitude vibration. Which data for training is described in **Table 2**, and data for prediction and verification of prediction results are described in **Table 3**.

Table 1
The material composition of SCM440 steel

Chemical composition	C	Si	Mn	P	S	Cr	Mo
Ratio (%)	0.38−0.43	0.15−0.35	0.60−0.85	≤0.03	≤0.03	0.9−1.2	0.15−0.3

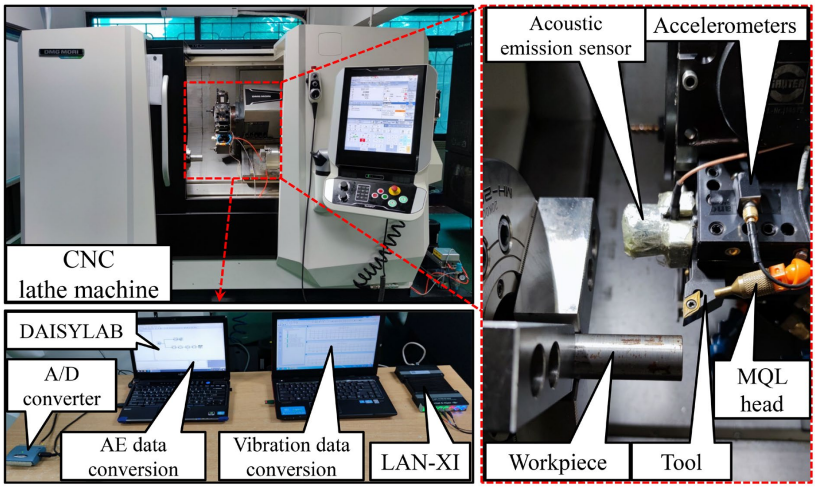

Fig. 1. Experimental setup for MQL turning SCM440 steel

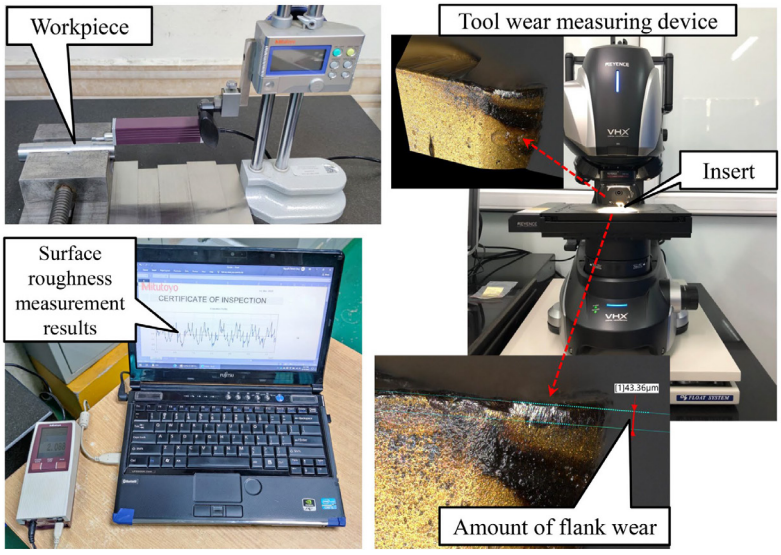

Fig. 2. Equipment for measuring surface roughness and tool wear

Table 2
Level of technological parameters when MQL turning

Technological characteristic	Lever 1	Level 2	Level 3
P – Injection pressure MQL [kgF/cm^3]	1.5	4	6.5
V – Cutting speed [m/min]	100	130	160
f – Feed rate [mm/rev]	0.05	0.1	0.15
t – Depth of cut (mm)	0.1	0.3	0.5

Table 3
Experimental results with measurement results of vibration amplitude, AE frequency and surface roughness

Experiment order	MQL condition *P*	Cutting speed *V*	Feed rate *f*	Depth of cut *t*
1	2	1	2	2
2	2	2	2	2
3	2	3	2	2
4	2	2	1	2
5	2	2	2	2
6	2	2	3	2
7	2	2	2	1
8	2	2	2	2
9	2	2	2	3
10	1	2	2	2
11	2	2	2	2
12	3	2	2	2

3. Results and discussion

3. 1. Experimental results

Vibration and AE signals are analyzed to identify various states, including machined surface roughness and tool wear. The results of direct measurements of flank wear, surface roughness and chip formation are used to verify the signals' response, thereby providing more precise tool wear monitoring, quality surface and surface. Experimental results in **Fig. 3** show that the surface quality changes under different cutting conditions.

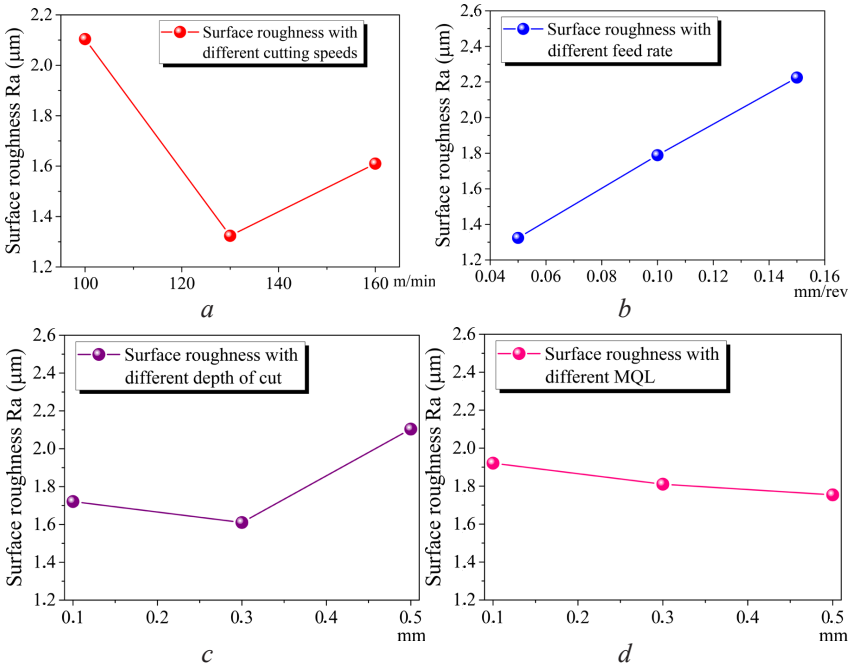

Fig. 3. The surface quality under different machining conditions:
a – surface roughness under the different cutting speeds; *b* – surface roughness under the different feed rates; *c* – surface roughness under the different deep of cut;
d – surface roughness under the different injection pressure MQL

The results in **Fig. 3, *a*** show that the surface quality is significantly improved when increasing the cutting speed from 100 m/min to 130 m/min. If continuing to grow the cutting speed to 160 m/min, the surface roughness tends to increase. When changing feed rate to surface quality, as depicted in **Fig. 3, *b***, shows that with increasing feed rate, the surface quality decreases. The effect of the feed rate on the surface quality is depicted as shown in **Fig. 3, *b***. The results show

that the surface quality decreases as the feed rate increases. **Fig. 3, *c*** shows the effect of depth of cut on surface quality. As the depth of cut was increased from 0.1 mm to 0.3 mm, the surface quality improved, however insignificantly. While increasing the depth of cut to 0.5 mm, surface roughness increased rapidly. The description in **Fig. 3, *d*** shows that when the MQL injection pressure is increased, the quality of the machined surface is improved.

The amount of flank wear after 20 min of machining with each tool under different machining conditions is depicted in **Fig. 4**.

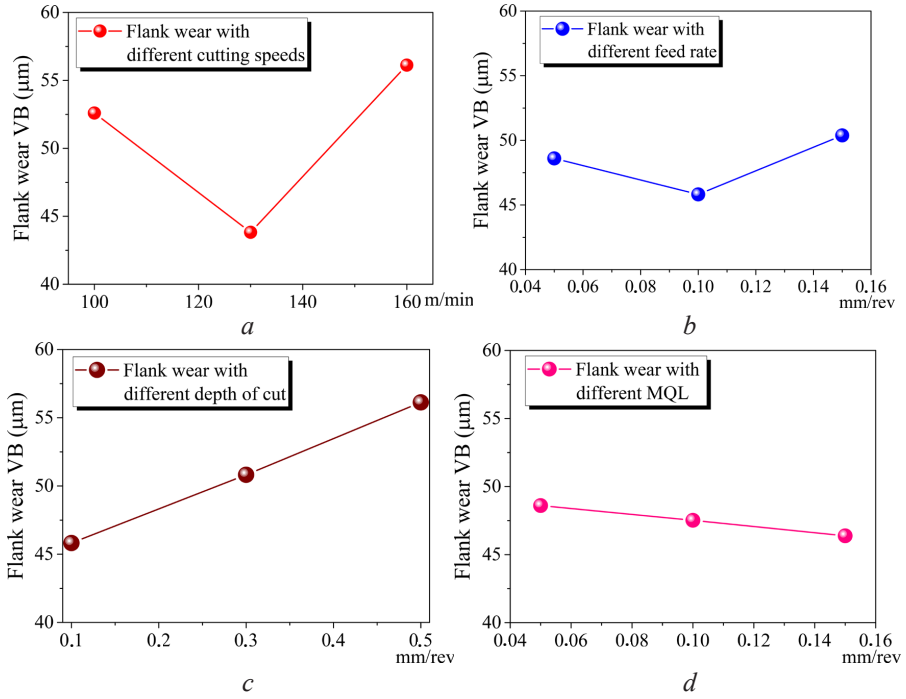

Fig. 4. Flank wears under different machining conditions:
a – VB under the different cutting speeds; *b* – VB under the different feed rates; *c* – VB under the different deep of cut; *d* – VB under the different injection pressure MQL

The results in **Fig. 4, *a*** show that the tool wear decreases when the cutting speed increases from 100 m/min to 130 m/min. The wear increases when the cutting speed increases to 160 m/min. The effect of feed rate on tool wear is depicted in **Fig. 4, *b*** shows the influence of feed rate on flank wear to be the same as the cutting speed, i.e. as the feed rate increases from 0.05 mm/rev to 0.1 mm/rev, the flank wear decreases. Continuing to increase the feed rate to 0.15 mm/rev will increase the amount of flank wear. However, the impact of the feed rate on tool wear is less than the cutting speed. The depiction in **Fig. 4, *c*** shows that the amount of tool wear increases with the increasing depth of cut. Meanwhile, the description in **Fig. 4, *d*** shows that with increasing MQL injection pressure, the amount of flank wear decreases.

Aim to study the relationship between technological parameters when using MQL turning (X) and output parameters, including surface quality and tool wear $Y(X)$ and $Z(X)$. The experimental results parameters as described in **Tables 2**, **3**. The scatter plot of the data is shown in **Fig. 5**. The data and the best-fit regression line are also given with the results of the data analysis and the input and the output from this program are given in **Fig. 5**, **Tables 4**, **5**.

Regression equations for surface quality and tool wear can be written according to cutting mode parameters when turning MQL:

$$Ra = 1.832248 - 0.044 \times P - 0.00823 \times V + 9.0067 \times f + 0.9575 \times t; \quad (1)$$

$$VB = 33.946 - 0.404 \times P + 0.058667 \times V + 17.8 \times f + 25.75 \times t. \quad (2)$$

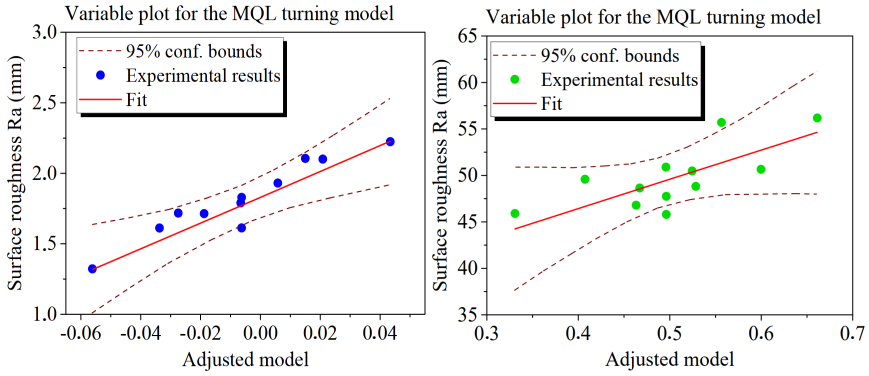

a *b*

Fig. 5. Fitted regression line for MQL turning technology parameter data: *a* – surface roughness; *b* – tool wear

Table 4

A simple linear regression model for the MQL turning cutting mode and surface roughness

Intercept	Coefficients	Standard Error	Lower 95 %	Upper 95 %
	1.832248	**0.758174**	**0.039451**	**3.625044**
MQL condition *P*	−0.044	0.057566	−0.18012	0.092121
Cutting speed *V*	−0.00823	0.004797	−0.01958	0.00311
Feed rate *f*	9.0067	2.878277	2.200657	15.81274
Depth of cut *t*	0.9575	0.719569	−0.74401	2.659011

Table 5

A simple linear regression model for the MQL turning cutting mode and tool wear

Intercept	Coefficients	Standard Error	Lower 95 %	Upper 95 %
	33.946	**14.60695**	**−0.59395**	**68.48595**
MQL condition *P*	−0.404	1.109056	−3.0265	2.2185
Cutting speed *V*	0.058667	0.092421	−0.15987	0.277208
Feed rate *f*	17.8	55.45278	−113.325	148.925
Depth of cut *t*	25.75	13.86319	−7.03125	58.53125

3. 2. Acoustic emission and vibration sensor signals in machining condition monitoring

The sensor signals obtained during machining describe the changes occurring in the material dynamics through their influence on the tool condition, and surface quality will be expressed in the analogue signal. The signals received by the sensor must be analyzed to investigate the tool condition, surface quality, and other monitoring conditions.

The received signals are the outstanding results of phenomena occurring in the machining process, which are very complex and random. From experimental procedures, the raw AE signals represent all phenomena produced by changes in the internal structure of the machined material. The results of the RMS analysis represent the energy content of the different signal components with the density of the respective occurrences. In normal turning processes, some significant phenomena such as plastic deformation, tool wear, chipping, tool breakage, and chip formation significantly influence the tool's working state and are represented through the received AE signal.

As shown in **Fig. 6, 7**, the AE and vibration signals were performed at a cutting speed of 100 m/min, a depth of cut of 0.05 mm and a feed rate of 0.1 mm/rev. **Fig. 6** show two AE signals with a continuous low-amplitude and a transient high-amplitude model. The constant low amplitude patterns of the AE signal are caused by plastic deformation and tool wear. In contrast, the temporary marks are caused by chip formation, chip breakage, and tool breakage. The vibration components depicted in **Fig. 7** also had similar pattern forms in AE analysis. Low amplitude signals are most

likely due to machine tool vibration. At the same time, the different appearance during machining is the source of the high amplitude signal pattern. Surface roughness changes, tool wear, chip formation patterns, collisions between the chip and the cutting tool during machining, disturbances in lubrication, and so on are the leading causes of frequency amplitude of oscillation with high frequency. **Fig. 8** represents the RMS of the vibration and AE signals from the original raw signals.

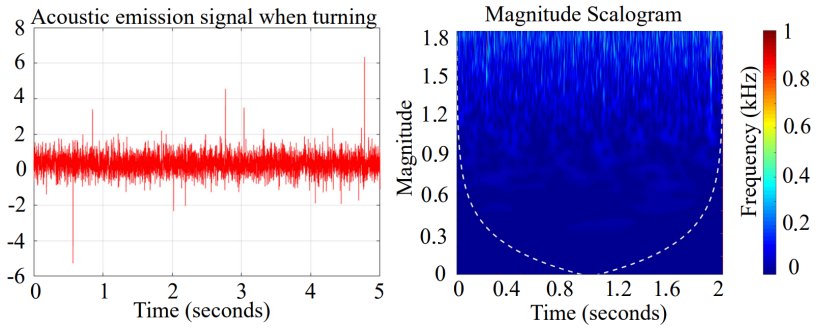

a *b*

Fig. 6. Acoustic emission signal when turning: *a* – AE signal; *b* – AE magnitude frequency

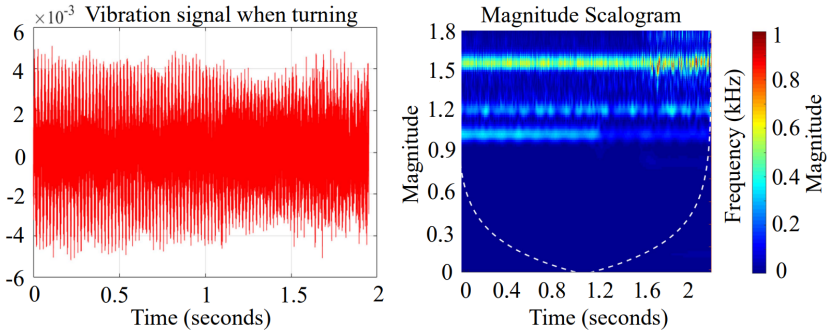

a *b*

Fig. 7. Vibration signal when turning: *a* – Vibration signal; *b* – Vibration magnitude frequency

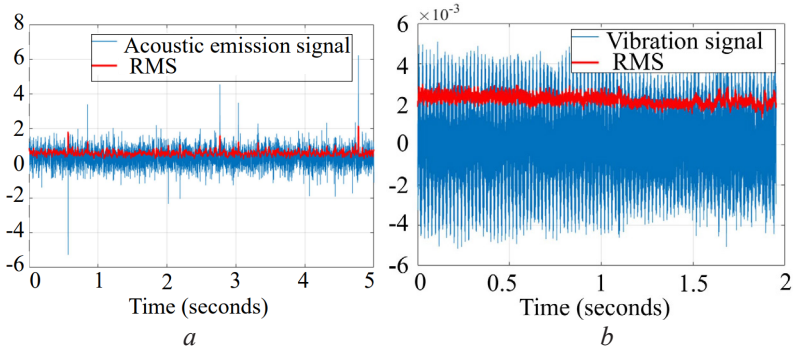

a *b*

Fig. 8. RMS of AE and vibration signals: *a* – RMS of AE signals; *b* – RMS of vibration signals

3. 3. Root mean square value of acoustic emission and vibration signals with different cutting modes

Root mean square value (RMS) amplitudes from AE and vibration sensor signals with different cutting conditions observing to find the relationship between tool conditions and surface roughness. The results in **Fig. 9** show the variation of RMS values at three different cutting speeds, from 100 m/min to 160 m/min, at three feed rates from 0.05 mm/rev to 0.15 mm/rev and at three cutting depths of 0.1 mm, 0.3 mm and 0.5 mm respectively keeping the other two conditions constant.

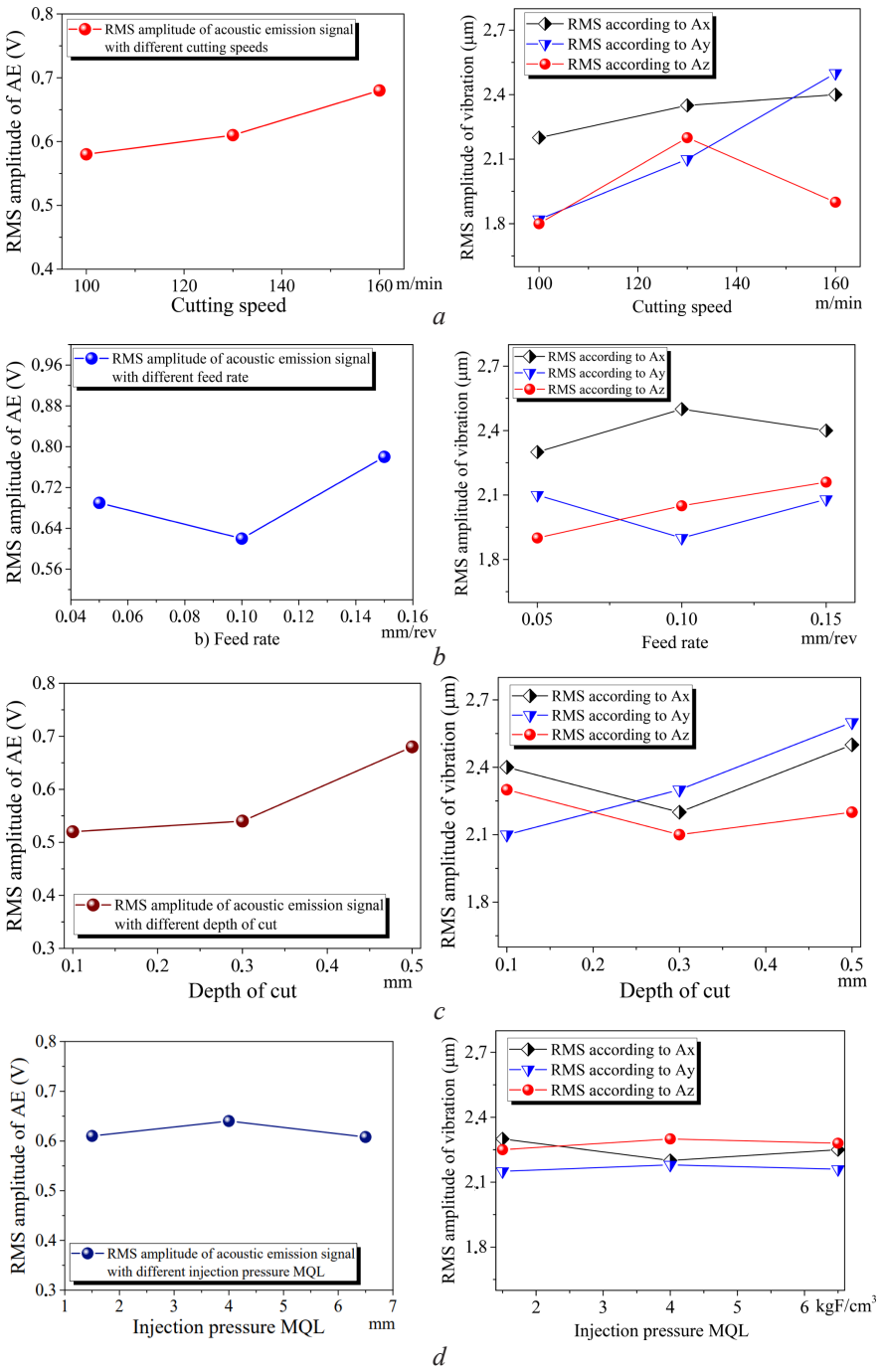

Fig. 9. RMS variation of AE and vibration amplitude signal with different machining conditions: *a* – cutting speed; *b* – feed rate; *c* – depth of cut; *d* – injection pressure

The amplitude of the RMS with the AE signal observed in **Fig. 9, *a*** is increased with the cutting speed from 100 m/min to 160 m/min. The results observed were differences between the propensity to wear tools, as depicted in **Fig. 4, *a***. Given the RMS amplitude of the AE signal at a shear rate of 130 m/min, the flank wear decreases abruptly even at higher shear rates. The survey results of the chips obtained in the tests showed that fracture, as described in **Fig. 10, *a*** may be responsible for the reduced tool wear. With chip breaking, stress develops in the cutting mode. The tool and workpiece contact is released, resulting in reduced tool wear and no corresponding decrease in RMS occurrence in the AE amplitude, as depicted in **Fig. 9, *a*, *b*** shows that the RMS amplitude of the AE signal decreases with a feed rate of 0.1 mm/rev. The fluctuations of RMS of

the AE signal are similar to the trend of flank wear, as depicted in **Fig. 4, *b***. The decrease in RMS signal and the decrease in flank wear can be caused by chip breakage occurring during machining, as described in **Fig. 10, *e***.

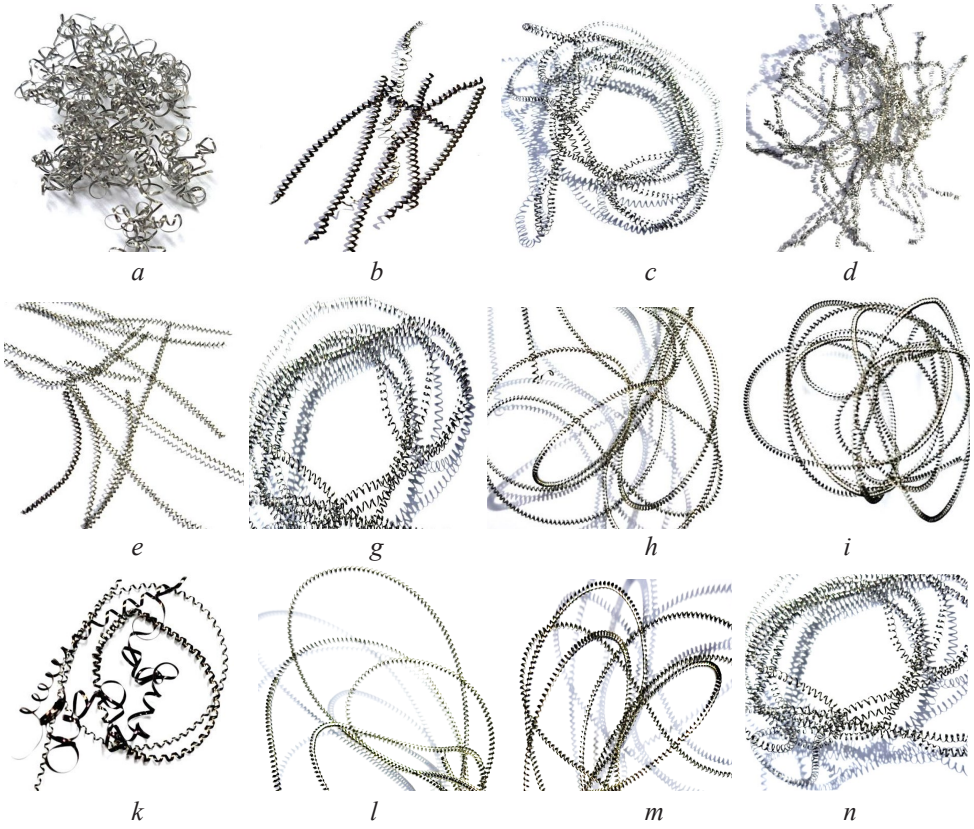

Fig. 10. Chip images under different machining conditions: *a* – Exp. 01; *b* – Exp. 02; *c* – Exp. 03; *d* – Exp. 04; *e* – Exp. 05; *g* – Exp. 06; *h* – Exp. 07; *i* – Exp. 08; *k* – Exp. 09; *l* – Exp. 10; *m* – Exp. 11; *n* – Exp. 12

The slight increase in the RMS trend of AE amplitude at 0.3 mm depth of cut and more pronounced at 0.5 mm, as shown in **Fig. 9, *c***, the corresponding increase in the histogram can be seen in flank wear **Fig. 4, *c***. The analysis in **Fig. 9, *d*** shows that the increase in MQL injection pressure is almost RMS of AE amplitude unchanged, similar to the trend of tool flank wear as shown by **Fig. 4, *d***, tool wear tends to decrease when pressure increases but not significantly. The analysis results show the consistency between the flank wear values and the RMS amplitude of the AE signal. In the case of cutting speed at 130 m/min, there is a difference in the trend between the RMS amplitude and the amount of tool wear due to chip breaking. Therefore, investigating the combination of AE signal RMS amplitude and chip image analysis for more accurate analysis.

3. 4. Experimentally confirm the tool wear prediction model and surface quality

In addition to the individual impact investigated, orthogonal experiments were investigated in addition to the particular effects investigated. The experiments set up by an orthogonal Table derive from association theory. Sequential experiments, as set up in **Table 3**, are the training data for the prediction process. Meanwhile, experiments were conducted according to Taguchi L27 empirical analysis to verify the ability to predict surface quality and tool wear, thereby confirming the correctness of the proposed model. Through experiment Taguchi L27, the design factors, including cutting speed, feed rate and depth of cut, are set in three levels. Injection pressure has a negligible effect on tool wear and surface quality and is set at level 3 in the experiments. The level of initial parameters of the experimental process is shown in **Table 2**, and the experiment sequence is

conducted according to the L27 orthogonal array. **Table 6** lists surface roughness, AE frequency, and instrument vibration experiment values.

Table 6
Experimental parameters according to Taguchi L27

Experimental parameters				Results of measuring surface quality and tool wear	
Exp. No.	**Cutting speed (*V*)**	**Feed rate (*S*)**	**Depth of cut (*t*)**	**Surface roughness (Ra)**	**Tool wear (*VB*)**
1	1	1	1	1.333	45
2	1	2	1	1.543	68
3	1	3	1	1.733	82
4	2	1	1	1.767	74
5	2	2	1	1.900	110
6	2	3	1	1.833	161
7	3	1	1	2.033	67
8	3	2	1	2.467	107
9	3	3	1	2.033	141
10	1	1	2	0.967	70
11	1	2	2	1.070	91
12	1	3	2	1.433	106
13	2	1	2	1.343	75
14	2	2	2	1.500	103
15	2	3	2	1.667	53
16	3	1	2	1.167	74
17	3	2	2	1.700	110
18	3	3	2	1.967	133
19	1	1	3	1.060	72
20	1	2	3	1.267	97
21	1	3	3	1.100	147
22	2	1	3	1.533	79
23	2	2	3	1.433	105
24	2	3	3	2.033	144
25	3	1	3	1.500	78
26	3	2	3	2.267	118
27	3	3	3	2.333	157

With the GPR-ANFIS hybrid algorithm, the authors hypothesized based on promoting and optimizing the advantages of the ANFIS model and the GPR model [19]. The generated model has an excellent ability to solve nonlinear functions and approximation problems combined with the ability to self-adjust the values of membership functions like in the ANFIS model. In addition, the generated model is a flexible and powerful tool that can provide both predictive results and confidence intervals of predictions as in GPR models. This unique combination, surface roughness and tool wear predictive value with training and test samples established by experimental data. The output parameters of the predictive model include surface quality and tool wear. Input parameters include cut-off factor, RMS analysis parameters, frequency domain from AE and vibration signals. The analysis results show superior predictive ability with an average prediction accuracy of 97.57 % with 98 % confidence.

The analysis results in **Fig. 11**, **12** show that the predicted surface roughness value is very close to the experimental result, with the highest prediction error less than 4.8 %. The ability to predict tool wear as described in **Fig. 13**, **14** also give a very close prediction to the measured value with an average error of 4.92 %. The obtained results show the stability as well as the reliability of the predictive model.

The input signals including cutting mode parameters, vibration and AE signals collected from sensors with the ability to extract signal features in 1 second, are fed into the neural system

in the GPR-ANFIS hybrid algorithm aims to provide results to predict surface quality and tool wear. The predicted model is set with CNC turning machining centre. A computer program processes the database, and the diagram of online monitoring of surface quality and tool wear is illustrated in **Fig. 15**.

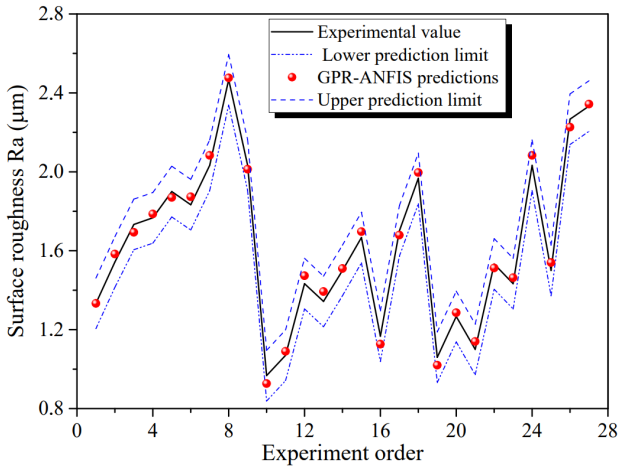

Fig. 11. Surface roughness prediction by GPR-ANFIS hybrid algorithm

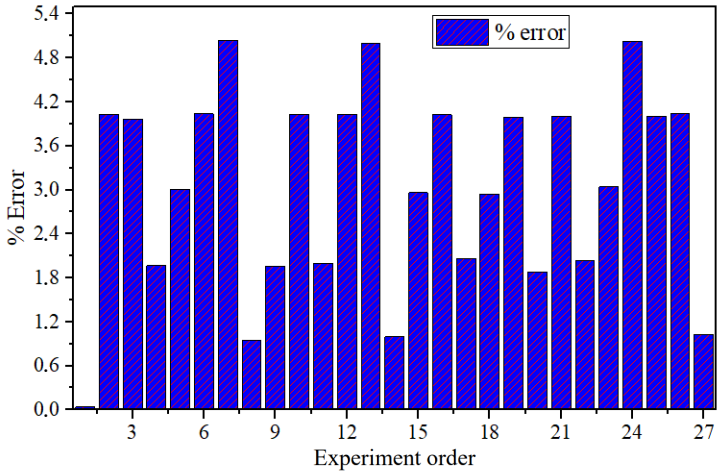

Fig. 12. Surface roughness prediction error by GPR-ANFIS hybrid algorithm

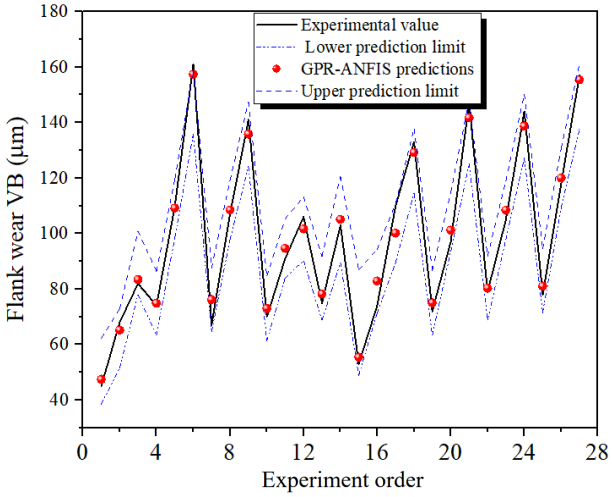

Fig. 13. Tool wear prediction by GPR-ANFIS hybrid algorithm

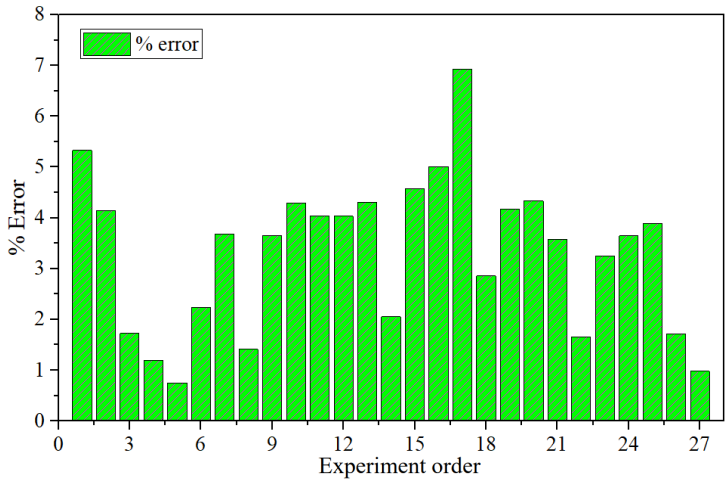

Fig. 14. Tool wear prediction error by GPR-ANFIS hybrid algorithm

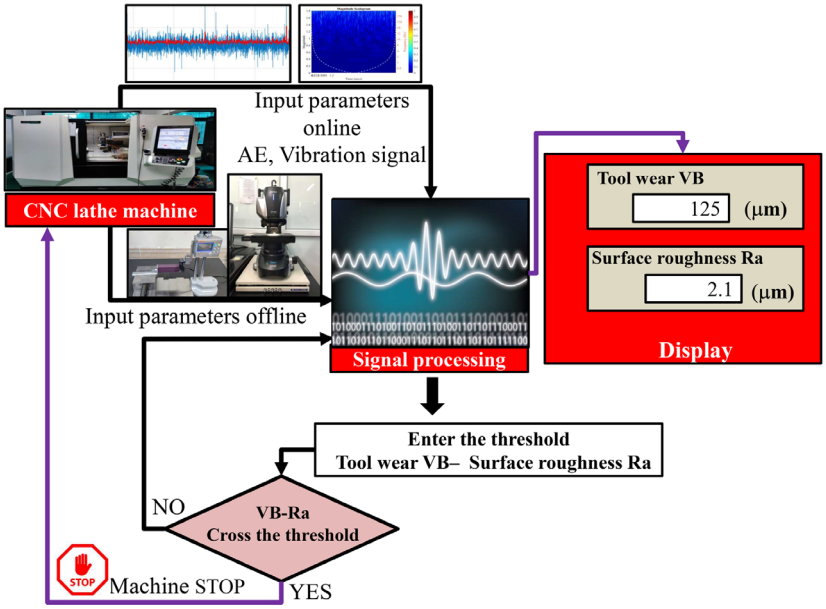

Fig. 15. Experimental diagram for online monitoring of CNC turning process

Suppose the monitoring parameters are predicted to be less than the allowable value. In that case, the machining process is continued for the next 1 second. When the predicted parameters are close to the threshold, the alarm device immediately sounds, alerting the user. If the parameters exceed the threshold, immediately, the alarm device works. At the same time, the machining centre returns the cutting tool to the original position and stops the machining process.

3. 5. Discussion

The above analysis shows that the AE and vibration signals cannot sense the entire range of the frequency domain. AE sensors capture high-frequency signals due to plastic deformation of the material, micro-cracking of the workpieces, tool fracture and chip breakage, while vibration sensors collect the signals with the low-frequency corresponding effect that occurs during machining. Therefore, combining AE and vibration sensors can confirm machining problems more accurately and completely.

The AE and vibration signals received from the sensors need to be processed and analyzed to obtain the necessary information. To achieve the most effective cutting tool condition monitoring the received signals must exhibit high sensitivity to tool conditions and low sensitivity to process parameters. The AE and vibration signals obtained during machining exist in complex waveforms. They consist of many fundamental signals coming from different occurrences. Further processing

is required to extract useful features for instrument condition monitoring based on the received signals. The vibration and AE signals are obtained digitally with FFT analysis allowing the conversion of time-domain data to frequency spectrum easy. The goal of the FFT is to get a frequency of the original signal that can be detected with the correlation features best suited to the cutting tool conditions. Therefore, the signal components obtained from the AE sensor and the vibration signal, together with the frequency analysis, can characterize different tooling conditions during turning.

The experimental results show that the RMS amplitude variation of the observed vibrational components is quite synthetic. The degree of vibration increases with the increase of cutting speed, feed rate and depth of cut. The results also show that *Az*, *Ax*, and *Ay* components respond to the RMS of the AE signal when cutting mode factors (variable cutting speed, feed rate and depth of cut) change accordingly. This shows that the vibration components *Ax*, *Ay* and *Az* are sensitive to the change in cutting conditions.

The AE and vibration signal components' amplitudes and frequency domain were recorded after the first 20 min of machining under different cutting conditions. The flank wear and surface roughness were measured, and chips were collected to correlate with fluctuations in the signal amplitude. The chip parameters are as shown in **Fig. 10**. With the increase of the cutting speed, the chips are observed to gradually change from the turbulent state to the cyclic type, while for increased feed rate, the detected chips vary from crumb to wire and curl type. Meanwhile, to increase the depth of cut, the chips changed from the coiled wire type to the side coil type. When increasing the injection pressure of MQL, the chip shape is almost unchanged.

The change in surface roughness is evident due to oscillation. Meanwhile, observing that the chip formation pattern affects tool wear. The fluctuations of the vibrating components can effectively describe the chip formation pattern. Trends of vibration components illustrate the effect of cutting conditions on tool wear. Although the entire signal range seems to be within a limit, the peak values, i.e. frequency of magnitude oscillations at different cutting speeds, feed rates and depth of cut. These findings are significant for cutting tool health monitoring, helping make machining processes safe and efficient. Tool wear information will help save on early removal costs and additional power consumption due to overuse of the cutting tool. Meanwhile, surface roughness information can help manufacturers find an optimal cutting condition for process machining. Frequency domain analysis will enhance investigation by identifying different occurrences in frequency more accurately than information obtained from time-domain signals.

The data analysis method and findings show the relationship between the AE and vibration signals and the tool condition parameters such as tool wear, surface roughness, chips etc. when MQL turning SCM440 material has not been studied. The AE signal and vibration amplitude work well to monitor tool conditions and various turning problems. The combined application of AE and vibration sensor has described tool wear, tool breakage, chip formation, chip breakage, machine tool vibration, workpiece surface roughness, etc. The vibration and AE signals and their frequency analysis can deduce a specific ratio at turning without any ambiguity.

A computer program processes the database illustrated in Fig. 15 and shows the input signals, including the cutting mode parameters, the proposed cutting force determination model and the vibration signals collected from the sensors with the ability to extract the signal features for 1 s, are used as input to the system neurons in the GPR-ANFIS hybrid algorithm to provide predictive results. The parameters obtained during MQL turning and sensor data are continually added to the prediction and optimization database during machining. The data set used in monitoring and optimization is set as follows. The initial data obtained from the sensors and the predicted and optimized parameters are removed. Data on surface quality and tool wear obtained from sensors are used as input to the neural networks and retrained with the updated training data sets. After changing the cutting tool, the neural network is retrained to predict surface roughness values and tool wear.

In subsequent studies, the authors elucidate the effect of the raw AE signal performing better or worse than RMS in investigating tool status and define different occurrences when turning complex. Along with that, more and more experimental studies were conducted aimed at understanding chip formation and the effect of wavelet analysis on the basis of combining AE and vibration signal decomposition when turning and milling surfaces with complex forms.

4. Conclusions

In this work, the experimental and analytical results show that the obtained AE and vibration signal components can effectively monitor various circumstances in the SCM440 steel turning process with MQL. The main findings from the study are described as follows:

− the analysis results show the consistency between the flank wear values and the RMS amplitude of the AE signal. In the case of cutting speed at 130 m/min, there is a difference in the trend between the RMS amplitude and the amount of tool wear due to chip breaking. Therefore, investigating the combination of AE signal RMS amplitude and chip image analysis for more accurate analysis;

− the type of chip formation affects tool wear; The oscillations of the vibrating components can effectively describe the chip formation pattern, while the trends of the vibrating components are capable of illustrating the effect of the cutting condition on tool wear;

− the effect of vibration on tool wear is maximum for curved chip forming up and down faces, decreasing gradually for laterally curved chip formation and curled chip formation. The degree of vibration increases with the increase of cutting speed, feed rate and depth of cut. The results also show that *Az*, *Ax*, and *Ay* components respond to the RMS of the AE signal when cutting mode factors (variable cutting speed, feed rate and depth of cut) change accordingly. This shows that the vibration components *Ax*, *Ay* and *Az* are sensitive to the change in cutting conditions;

− the analysis results show superior predictive ability with an average prediction accuracy of 97.57 % with 98 % confidence. The predicted surface roughness value is very close to the experimental result, with the highest prediction error of less than 4.8 %. The ability to predict tool wear is very close to the measured value, with an average error of 4.92 %. The obtained results show the stability as well as the reliability of the predictive model;

− provide a turning model from the control point of view. This model and related conceptual system are suiTable for the requirements of adaptive control and online monitoring of surface quality and tool wear. The system has been successfully tested, meeting the monitoring requirements in practice.

Correlation of the AE signal and vibration signature with various incidents such as tool wear, surface roughness and chip formation during rotation can effectively determine the condition of the cutting tool. This will help the process to monitor the tool condition without interrupting the process.

Conflict of Interest

The authors declare that there is no conflict of interest in relation to this paper, as well as the published research results, including the financial aspects of conducting the research, obtaining and using its results, as well as any non-financial personal relationships.

Financing

The study was performed without financial support.

Data availability

Data will be made available on reasonable request.

Acknowledgements

The work described in this paper was supported by Ha Noi University of Industry (HaUI, Vietnam) for a scientific project.

References

[1] Zhang, N., Komoda, R., Yamada, K., Kubota, M., Staykov, A. (2022). Ammonia mitigation and induction effects on hydrogen environment embrittlement of SCM440 low-alloy steel. International Journal of Hydrogen Energy, 47 (33), 15084–15093. doi: https://doi.org/10.1016/j.ijhydene.2022.03.006

[2] Kwak, J.-S., Sim, S.-B., Jeong, Y.-D. (2006). An analysis of grinding power and surface roughness in external cylindrical grinding of hardened SCM440 steel using the response surface method. International Journal of Machine Tools and Manufacture, 46 (3-4), 304–312. doi: https://doi.org/10.1016/j.ijmachtools.2005.05.019

[3] Thien, N. V., Trung, D. D. (2021). Study on model for cutting force when milling SCM440 steel. EUREKA: Physics and Engineering, 5, 23–35. doi: https://doi.org/10.21303/2461-4262.2021.001743

[4] Tazoe, K., Hamada, S., Noguchi, H. (2017). Fatigue crack growth behavior of JIS SCM440 steel near fatigue threshold in 9-MPa hydrogen gas environment. International Journal of Hydrogen Energy, 42 (18), 13158–13170. doi: https://doi.org/10.1016/j.ijhydene.2017.03.223

[5] Chen, C.-C., Liu, N.-M., Chiang, K.-T., Chen, H.-L. (2012). Experimental investigation of tool vibration and surface roughness in the precision end-milling process using the singular spectrum analysis. The International Journal of Advanced Manufacturing Technology, 63 (5-8), 797–815. doi: https://doi.org/10.1007/s00170-012-3943-4

[6] Thirumalai, R., Srinivas, S., Vinodh, T., Kowshik Kumar, A. L., Kumar, M. K. (2014). Optimization of Surface Roughness and Flank Wear in Turning SCM440 Alloy Steel Using Taguchi Method. Applied Mechanics and Materials, 592-594, 641–646. doi: https://doi.org/10.4028/www.scientific.net/amm.592-594.641

[7] Thamizhmanii, S., Hasan, S. (2009). Effect of tool wear and forces by turning process on hard AISI 440 C and SCM 440 materials. International Journal of Material Forming, 2 (S1), 531–534. doi: https://doi.org/10.1007/s12289-009-0429-5

[8] Jeong, J.-I., Kim, J.-H., Choi, S.-G., Cho, Y. T., Kim, C.-K., Lee, H. (2021). Mechanical Properties of White Metal on SCM440 Alloy Steel by Laser Cladding Treatment. Applied Sciences, 11 (6), 2836. doi: https://doi.org/10.3390/app11062836

[9] Kong, Y. S., Cheepu, M., Lee, J.-K. (2021). Evaluation of the mechanical properties of Inconel 718 to SCM 440 dissimilar friction welding through real-time monitoring of the acoustic emission system. Proceedings of the Institution of Mechanical Engineers, Part L: Journal of Materials: Design and Applications, 235 (5), 1181–1190. doi: https://doi.org/10.1177/1464420721993838

[10] Furuya, Y., Matsuoka, S., Abe, T. (2003). A novel inclusion inspection method employing 20 kHz fatigue testing. Metallurgical and Materials Transactions A, 34 (11), 2517–2526. doi: https://doi.org/10.1007/s11661-003-0011-6

[11] Panda, D., Kumari, K., Dalai, N. (2022). Performance of Minimum Quantity Lubrication (MQL) and its effect on Dry Machining with the addition of Nano-particle with the biodegradable base fluids: A review. Materials Today: Proceedings, 56, 1298–1301. doi: https://doi.org/10.1016/j.matpr.2021.11.275

[12] Gaurav, G., Sharma, A., Dangayach, G. S., Meena, M. L. (2020). Assessment of jojoba as a pure and nano-fluid base oil in minimum quantity lubrication (MQL) hard-turning of Ti–6Al–4V: A step towards sustainable machining. Journal of Cleaner Production, 272, 122553. doi: https://doi.org/10.1016/j.jclepro.2020.122553

[13] Özbek, N. A., Çiçek, A., Gülesin, M., Özbek, O. (2016). Effect of cutting conditions on wear performance of cryogenically treated tungsten carbide inserts in dry turning of stainless steel. Tribology International, 94, 223–233. doi: https://doi.org/10.1016/j.triboint.2015.08.024

[14] Tran, N.-H., Park, H.-S., Nguyen, Q.-V., Hoang, T.-D. (2019). Development of a Smart Cyber-Physical Manufacturing System in the Industry 4.0 Context. Applied Sciences, 9 (16), 3325. doi: https://doi.org/10.3390/app9163325

[15] Hozdić, E. (2015). Smart factory for industry 4.0: A review. Journal of Modern Manufacturing Systems and Technology, 7 (1), 28–35. Available at: https://www.researchgate.net/publication/282791888_Smart_factory_for_industry_40_A_review

[16] Usca, Ü. A., Uzun, M., Şap, S., Kuntoğlu, M., Giasin, K., Pimenov, D. Y., Wojciechowski, S. (2022). Tool wear, surface roughness, cutting temperature and chips morphology evaluation of Al/TiN coated carbide cutting tools in milling of Cu-B-CrC based ceramic matrix composites. Journal of Materials Research and Technology, 16, 1243–1259. doi: https://doi.org/10.1016/j.jmrt.2021.12.063

[17] Wu, Q., Chen, G., Liu, Q., Pan, B., Chen, W. (2022). Investigation on the Micro Cutting Mechanism and Surface Topography Generation in Ultraprecision Diamond Turning. Micromachines, 13 (3), 381. doi: https://doi.org/10.3390/mi13030381

[18] Orhan, S., Er, A. O., Camuşcu, N., Aslan, E. (2007). Tool wear evaluation by vibration analysis during end milling of AISI D3 cold work tool steel with 35 HRC hardness. NDT & E International, 40 (2), 121–126. doi: https://doi.org/10.1016/j.ndteint.2006.09.006

[19] Nguyen, D., Yin, S., Tang, Q., Son, P. X., Duc, L. A. (2019). Online monitoring of surface roughness and grinding wheel wear when grinding Ti-6Al-4V titanium alloy using ANFIS-GPR hybrid algorithm and Taguchi analysis. Precision Engineering, 55, 275–292. doi: https://doi.org/10.1016/j.precisioneng.2018.09.018

Received date 22.07.2022
Accepted date 08.12.2022
Published date 19.01.2023

How to cite: *Hoang, D. T., Thien, N. V., Pham, T. T. T., Nguyen, T. D. (2023). Combined analysis of acoustic emission and vibration signals in monitoring tool wear, surface quality and chip formation when turning SCM440 steel using MQL. EUREKA: Physics and Engineering, 1, 86–101. doi: https://doi.org/10.21303/2461-4262.2023.002509*